High-Affinity Nitrate Transport in Roots of Arabidopsis Depends on Expression of the *NAR2*-Like Gene *AtNRT3.1*[1]

Mamoru Okamoto, Anshuman Kumar[2], Wenbin Li, Ye Wang, M. Yaeesh Siddiqi, Nigel M. Crawford, and Anthony D.M. Glass*

Section of Cell and Developmental Biology, Division of Biological Sciences, University of California at San Diego, La Jolla, CA 92093–0116 (M.O., N.M.C.); and Department of Botany, University of British Columbia, Vancouver, British Columbia, Canada V6T 1Z4 (A.K., W.L., Y.W., M.Y.S., A.D.M.G.)

The NAR2 protein of *Chlamydomonas reinhardtii* has no known transport activity yet it is required for high-affinity nitrate uptake. Arabidopsis (*Arabidopsis thaliana*) possesses two genes, *AtNRT3.1* and *AtNRT3.2*, that are similar to the *C. reinhardtii NAR2* gene. *AtNRT3.1* accounts for greater than 99% of *NRT3* mRNA and is induced 6-fold by nitrate. *AtNRT3.2* was expressed constitutively at a very low level and did not compensate for the loss of *AtNRT3.1* in two *Atnrt3.1* mutants. Nitrate uptake by roots and nitrate induction of gene expression were analyzed in two T-DNA mutants, *Atnrt3.1-1* and *Atnrt3.1-2*, disrupted in the *AtNRT3.1* promoter and coding regions, respectively, in 5-week-old plants. Nitrate induction of the nitrate transporter genes *AtNRT1.1* and *AtNRT2.1* was reduced in *Atnrt3.1* mutant plants, and this reduced expression was correlated with reduced nitrate concentrations in the tissues. Constitutive high-affinity influx was reduced by 34% and 89%, respectively, in *Atnrt3.1-1* and *Atnrt3.1-2* mutant plants, while high-affinity nitrate-inducible influx was reduced by 92% and 96%, respectively, following induction with 1 mM KNO_3 after 7 d of nitrogen deprivation. By contrast, low-affinity influx appeared to be unaffected. Thus, the constitutive high-affinity influx and nitrate-inducible high-affinity influx (but not the low-affinity influx) of higher plant roots require a functional *AtNRT3* (*NAR2*) gene.

Nitrate influx into plant roots has been defined kinetically as being composed of at least four additive fluxes; constitutive high-affinity influx (CHATS), nitrate-inducible high-affinity influx (IHATS), constitutive low-affinity influx (CLATS), and inducible low-affinity influx (ILATS; Crawford and Glass, 1998; Forde, 2000). Members of the *NRT2* family of transporters are involved in the IHATS in fungi, algae, and plants. The first members of this family were cloned from *Aspergillus nidulans* and *Chlamydomonas reinhardtii* (Unkles et al., 1991; Quesada et al., 1994) by use of mutants defective in nitrate transport. Sequence similarities among these genes enabled Trueman et al. (1996) to clone the first members of this family from plants (*HvNRT2.1* and *HvNRT2.2* from barley [*Hordeum vulgare*]). Subsequently, *AtNRT2.1* and *AtNRT2.2* were cloned from Arabidopsis (*Arabidopsis thaliana*; Filleur and Daniel-Vedele, 1999; Zhuo et al., 1999) along with similar genes from several other plant species (for review, see Crawford and Glass, 1998; Forde, 2000). Evidence that *NRT2* genes play an important role in high-affinity nitrate transport came first from strong correlations between *AtNRT2.1* and *AtNRT2.2* expression and high-affinity influx during induction by nitrate (Zhuo et al., 1999; Okamoto et al., 2003) and during down-regulation by various nitrogen sources (Vidmar et al., 2000; Nazoa et al., 2003). A T-DNA mutant of Arabidopsis disrupted in the *AtNRT2.1* and *AtNRT2.2* genes exhibited severe and specific impairment of IHATS function, providing further support for this idea (Cerezo et al., 2001; Filleur et al., 2001). However, in *C. reinhardtii NRT2* genes do not act alone; two high-affinity nitrate transporter genes (*CrNRT2.1* and *CrNRT2.2*) require a second gene, *CrNAR2*, to function in nitrate transport (Quesada et al., 1994). A role for *CrNAR2* in nitrate uptake was confirmed in Xenopus oocytes. Oocytes injected with *CrNAR2* or *CrNRT2.1* mRNA separately gave no evidence of nitrate transport activity, whereas coinjection of both mRNAs produced nitrate currents (Zhou et al., 2000). Similar results were reported for barley, where one of three *NAR2*-like genes, *HvNAR2.3*, is able to increase nitrate transport compared to water-injected Xenopus oocytes when coexpressed with *HvNRT2.1* (Tong et al., 2005). These findings indicate that NAR2 is not required for transcriptional regulation of *NRT2.1* but is, instead, facilitating NRT2.1 transport activity perhaps by a direct interaction.

The completion of the Arabidopsis genome-sequencing project enabled us to search for the presence of *NAR2*

[1] This work was supported by the Natural Sciences and Engineering Research Council of Canada (to A.D.M.G) and by the National Institutes of Health (grant no. GM40672 to N.M.C.).

[2] Present address: Department of Biology, Colorado State University, Fort Collins, CO 80525.

* Corresponding author; e-mail aglass@interchange.ubc.ca; fax 604–822–6089.

The author responsible for distribution of materials integral to the findings presented in this article in accordance with the policy described in the Instructions for Authors (www.plantphysiol.org) is: Anthony D.M. Glass (aglass@interchange.ubc.ca).

Article, publication date, and citation information can be found at www.plantphysiol.org/cgi/doi/10.1104/pp.105.074385.

genes in this plant. Two such *NAR2*-like genes were found. We propose to name them *AtNRT3.1* and *AtNRT3.2*, respectively, since *NAR* is already reserved for another gene in Arabidopsis. We obtained two T-DNA insertion mutants for *AtNRT3.1*, one disrupted in the promoter region and the other in the coding region. These mutants were used to investigate whether high-affinity nitrate transport in Arabidopsis requires *NRT3* function in planta.

RESULTS

Identification of the *AtNRT3* Gene Family

Two genes in Arabidopsis were revealed by a homology search against the Arabidopsis genome database (Arabidopsis Genome Initiative, 2000) using the *C. reinhardtii* NAR2 sequences, namely, *AtNRT3.1* (GenBank ID: AJ310933; Arabidopsis Genome Initiative [AGI] code: At5g50200) and *AtNRT3.2* (GenBank ID: BX842351; AGI code: At4g24720). Predicted open reading frames of *AtNRT3.1* and *AtNRT3.2* encode 210 and 209 amino acids, respectively, sharing 61% identity and 76% similarity with each other (Fig. 1A). SignalP (Nielsen et al., 1999) and PSORT (Nakai and Kanehisa, 1992) predict that both AtNRT3 proteins possess signal peptides, with a predicted cleavage site between amino acids 22 and 23. One transmembrane region was predicted at the C terminus, leaving a long hydrophilic N-terminal end that is predicted to be extracellular.

Isolation of *Atnrt3* Mutants

To find a T-DNA insertion in *AtNRT3.1*, a PCR-based screen was carried out with a population of 60,480 T-DNA insertion lines (ecotype Wassilewskija [Ws] background) from the Arabidopsis knockout facility at the University of Wisconsin (see "Materials and Methods" for details). A T-DNA insertion line was isolated, and sequence analysis of the T-DNA-genomic DNA junction regions revealed that the insertion was 184 bp upstream from the predicted start codon of *AtNRT3.1*; there was a deletion of 51 bp of genomic DNA (−185 to approximately −235) and both 5′ and 3′ ends of the T-DNA were right borders, predicting two copies of T-DNA in a tandem inverted orientation. This T-DNA line was designated as *Atnrt3.1-1* (Fig. 1B).

Another putative *Atnrt3.1* mutant was identified in the FLAGdb T-DNA lines (Samson et al., 2002). PCR analysis with respective primers of *AtNRT3.1* genomic DNA and the T-DNA confirmed a T-DNA insertion near the end of the gene. The T-DNA insertion started at 858 bp from the start codon, deleting 66 bp of exon 2 and 5 bp of the 3′ untranslated region. This second mutant was designated as *Atnrt3.1-2* (Fig. 1B).

The T-DNA mutants were backcrossed twice to wild type (ecotype Ws) and the resulting homozygous lines were used for further investigation. To determine T-DNA copy number, Southern-blot and relative quantitative real-time PCR analyses were carried out (Fig. 1, C and D). For Southern-blot analysis, genomic DNAs of *Atnrt3.1-1* and *Atnrt3.1-2* were digested with *Sal*I/*Sph*I and *Bam*HI, respectively, and hybridized with the T-DNA-specific probe (1.2 kb of *β-glucuronidase* (*GUS*) gene; Kaiser et al., 2002). The fragment sizes in the blot are similar to the predicted sizes (Fig. 1, B and C). *GUS* gene copy numbers were also determined by quantitative real-time PCR assay (Ingham et al., 2001). The results from both methods indicated that *Atnrt3.1-1* and *Atnrt3.1-2* carry two copies and one copy of T-DNA, respectively.

Expression of *AtNRT3.1* and *AtNRT3.2* in Wild-Type Plants and *Atnrt3.1* Mutants

Several expressed sequence tags (ESTs) and full-length cDNA sequence data of *AtNRT3.1* are published in The Arabidopsis Information Resource database (http://arabidopsis.org/), indicating that *AtNRT3.1* is indeed expressed in Arabidopsis plants, whereas no EST is available for *AtNRT3.2*. We analyzed the expression level of the two *AtNRT3* genes in wild-type roots that had been grown in 1 mM NH_4NO_3 for 4 weeks, followed by 1 week in 50 μM KNO_3 by real-time relative reverse transcription (RT)-PCR. Figure 2A shows relative expression levels of *AtNRT3.1* and *AtNRT3.2* genes against clathrin, a housekeeping gene (AGI code: At4g24550). Relative to clathrin, *AtNRT3.1* showed a much higher level of expression than *AtNRT3.2*, which was barely detectable. Several more gene-specific primer sets were employed to confirm these results (data not shown). This may explain the absence of an EST for *AtNRT3.2*, yet we were able to detect expression of this gene due to the sensitivity of the assay.

The expression profile of the *AtNRT3* genes was also examined in *Atnrt3* mutant plants. *AtNRT3.1* expression levels in roots of *Atnrt3.1-1* and *Atnrt3.1-2* mutants were reduced by 90% and 100%, respectively, compared to those of wild-type plants under the same conditions (i.e. 1 mM NH_4NO_3 for 4 weeks, followed by 1 week in 50 μM KNO_3). In *Atnrt3.1-1* shoots, levels of *AtNRT3.1* were roughly 1% to approximately 2% of those of wild-type roots, whereas in *Atnrt3.1-2* there was a complete absence of *AtNRT3.1* (Fig. 2B). These results demonstrate that *Atnrt3.1-1* is a knockdown mutant and *Atnrt3.1-2* is a knockout mutant. They also show that *AtNRT3.1* expression is much higher in roots than shoots (about 100-fold higher).

It is possible that *AtNRT3.2*, a homolog of *AtNRT3.1*, might have compensated for the loss of *AtNRT3.1* function in the *Atnrt3.1* mutants. However, expression levels of *AtNRT3.2* in roots and shoots of *Atnrt3.1* mutant plants remained at low levels, though somewhat higher than in wild-type roots (Fig. 2C).

Phenotypes of the *Atnrt3.1* Mutants and Restoration of Wild-Type Phenotype with an *AtNRT3.1* cDNA

There was no obvious phenotype when the *Atnrt3.1* mutants were grown in peat-based soil, but phenotypic

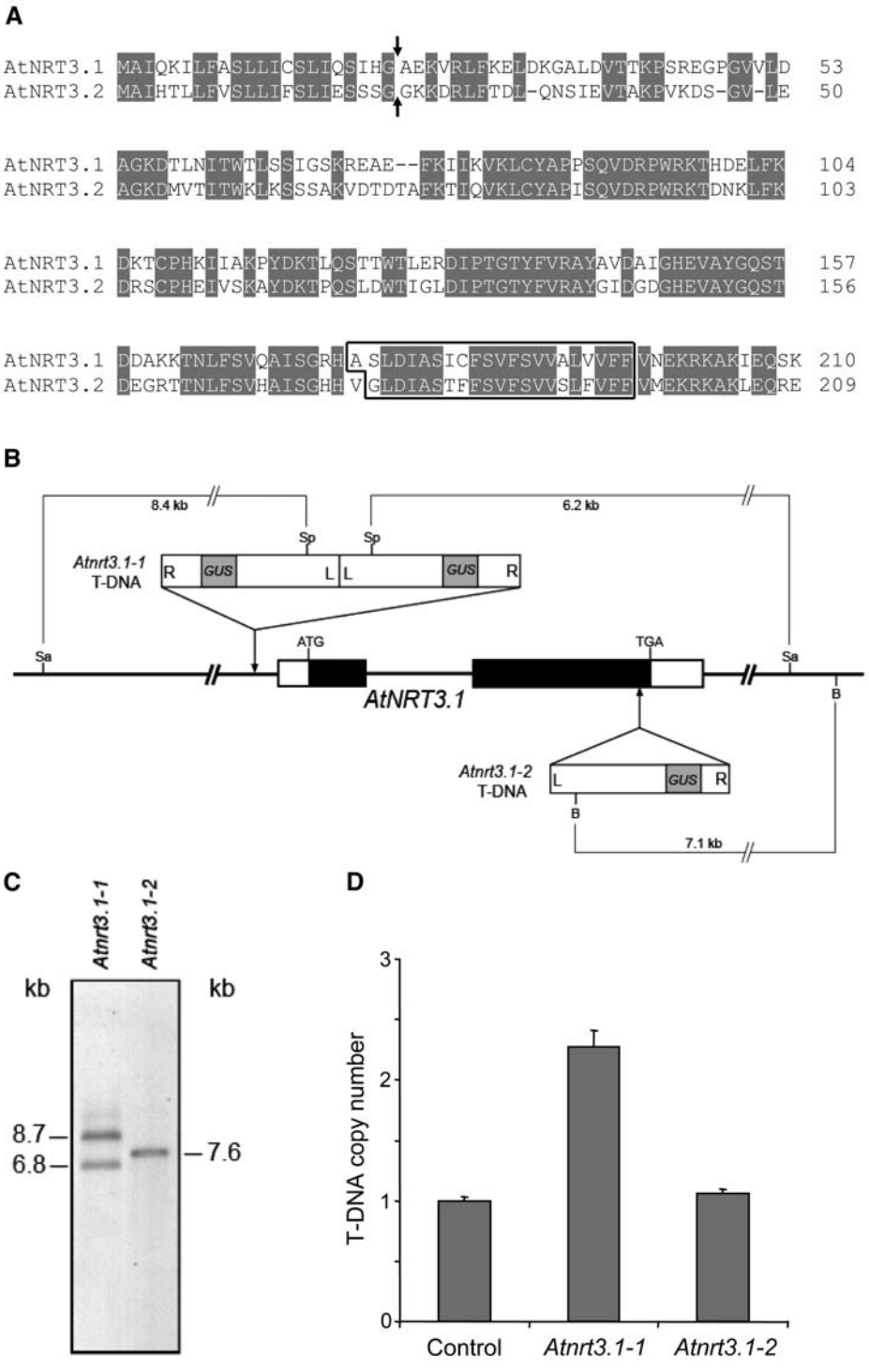

Figure 1. Amino acid sequences of AtNRT3 proteins and characterization of *Atnrt3.1* T-DNA lines. A, Amino acid sequence comparison of AtNRT3.1 and AtNRT3.2. Identical amino acids are shaded. Arrows indicate predicted cleavage sites. The transmembrane region predicted by TMHMM (Krogh et al., 2001) is boxed. B, Schematic diagram of *AtNRT3.1* with the T-DNA insertions. In *AtNRT3.1* white boxes indicate 5′ or 3′ untranslated region, and black boxes indicate open reading frame. The T-DNAs in the *Atnrt3.1-1* and *Atnrt3.1-2* mutants are inserted 186 bp upstream of the first putative start codon, and 63 bp before the stop codon, respectively. The diagram is not drawn in scale. R, Right border; L, left border; Sa, *Sal*I; Sp, *Sph*I; B, *Bam*HI. C, The Southern blot of the *Atnrt3.1* mutants. Genomic DNAs of *Atnrt3.1-1* and *Atnrt3.1-2* were digested with *Sal*I/*Sph*I and *Bam*HI, respectively, and probed with a 1.2-kb fragment of *GUS* gene (Kaiser et al., 2002). D, The T-DNA copy number in the *Atnrt3* mutants measured by relative quantitative real-time PCR. Each sample was normalized by nitrite reductase (a single copy gene, AGI code: At2g15620), and expressed relative to the control T-DNA line (M. Galli, unpublished data).

differences became apparent when external nitrogen sources were controlled. When grown on plates containing 250 μM NO_3^- as the sole source of available nitrogen for 10 d, mutant plants grew poorly, shoot growth being particularly affected (Fig. 3A). By contrast to these phenotypic differences, mutant growth was normalized when plants were grown on 2.5 mM NO_3^-, 500 μM NH_4NO_3, or 250 μM NH_4^+ as sole nitrogen sources (Fig. 3, B–D).

When mutants (both *Atnrt3.1-1* and *Atnrt3.1-2*) and wild-type plants were grown in a common tank containing 1 mM NH_4NO_3 for 4 weeks, followed by 1 week without a source of nitrogen, to deinduce the IHATS in preparation for influx measurements, shoot-to-root

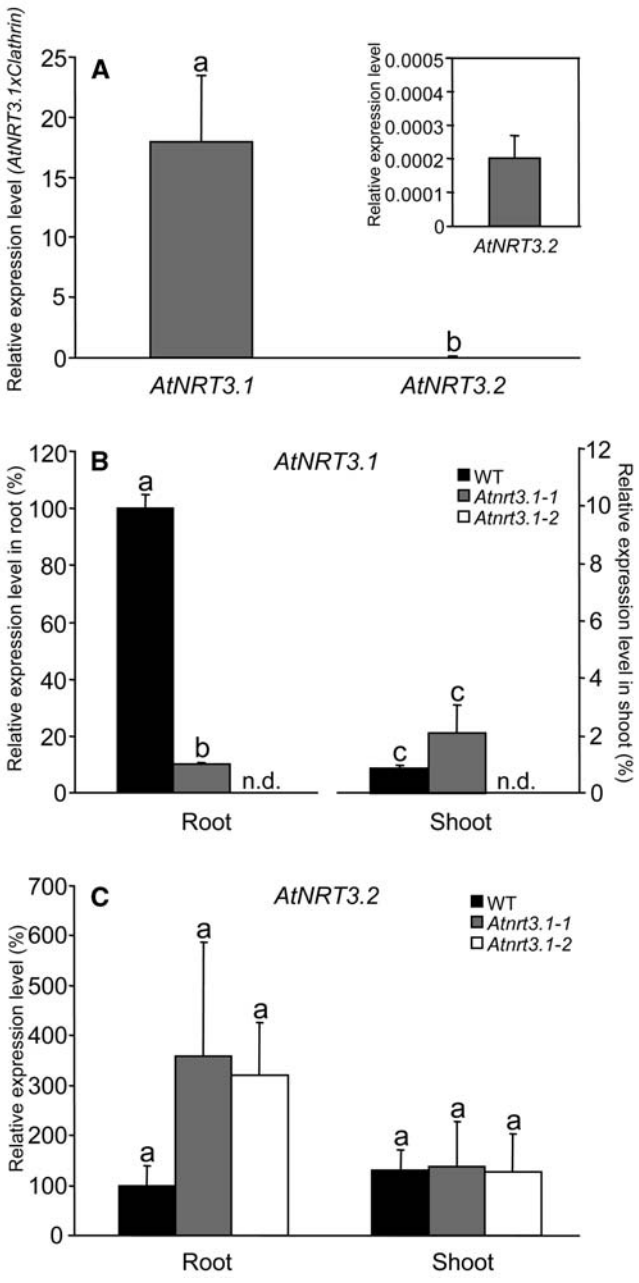

Figure 2. Expression analysis of *AtNRT3.1* and *AtNRT3.2* by relative quantitative real-time RT-PCR. Plants were grown for 4 weeks in 1 mM NH_4NO_3 and then transferred to 50 μM KNO_3 for 1 week. A, Relative expression level of *AtNRT3.1* and *AtNRT3.2* against clathrin, a housekeeping gene, in wild-type roots. The inset is an expanded-scale plot of *AtNRT3.2*. B and C, Relative expression profile of *AtNRT3.1* (B) and *AtNRT3.2* (C) in wild-type plants and *Atnrt3.1* mutants. Each sample was normalized by clathrin and relatively expressed to wild-type root. The values are means of four replicates (two biological replicates $\times$ two independent reactions). Error bars = SE. Different letters above the bars indicate significant difference at $P < 0.05$ (*t* test). n.d. indicates the following levels: root (<0.1%) and shoot (0%).

ratios were consistently and significantly lower ($P < 0.05$) in the mutant plants than in wild-type plants. Absolute values for shoot-to-root ratios varied from one experiment to another. Table I provides representative values for wild-type plants and *Atnrt3.1* mutants as well as shoot and root fresh weights (FWs). Shoot:root ratios were 3.5 (wild type), 1.4 (*Atnrt3.1-1*), and 1.5 (*Atnrt3.1-2*), respectively, differences that were highly significant ($P < 0.05$), as were shoot biomasses, but root weights were not different. However, in some experiments using older plants FWs of mutant roots were greater than those of wild-type plants (data not shown).

Genetic complementation of the two mutant lines by introducing a *AtNRT3.1* cDNA driven by the cauliflower mosaic virus (CaMV) 35S promoter (lines C1-3, C1-13, C2-2, and C2-5) restored their growth on 250 μM NO_3^- to that of wild-type plants (Fig. 3, E and F).

Nitrate Responses of *AtNRT3* and Nitrate Transporter Genes

The induction by nitrate of *AtNRT3* and the major nitrate transporter genes was examined in plants previously deprived of nitrogen and subsequently exposed to 1 mM KNO_3 for 3 or 6 h. Growth and nitrogen deprivation conditions were the same as used for the nitrate uptake experiments described below. Following this treatment, RNA was extracted and analyzed by relative real-time RT-PCR. In wild-type roots, *AtNRT3.1* was strongly induced by 1 mM KNO_3 (6-fold by 3 h); in shoots there is much less *AtNRT3.1* mRNA and little response to the same treatment (Fig. 4A). The *Atnrt3.1-1* mutant showed significantly less *AtNRT3.1* mRNA in roots prior to reexposure to KNO_3 (<40% of wild type), and no response to inducing conditions (1 mM KNO_3); shoots showed expression levels similar to those of the wild type. Compared to wild type (100%), the level of *AtNRT3.1* mRNA in the *Atnrt3.1-2* mutant was essentially 0% in both roots and shoots as expected for a null mutant. *AtNRT3.2* showed no consistent pattern of expression in wild-type and mutant plants except for a slight induction after 6 h in wild-type plants (Fig. 4B).

Two *NRT* nitrate transporters, a dual-affinity nitrate transporter, *AtNRT1.1* (*CHL1*) (Tsay et al., 1993; Wang et al., 1998; Liu et al., 1999; Liu and Tsay, 2003), and a high-affinity nitrate transporter, *AtNRT2.1*, were also analyzed under the same conditions as described above. In wild-type roots, both *AtNRT1.1* and *AtNRT2.1* were induced approximately 13- and 18-fold, respectively, by 1 mM KNO_3, peaking at 6 and 3 h, respectively (Fig. 4, C and D). *AtNRT1.1* mRNA levels were estimated to be 20- to 35-fold lower than those for *AtNRT2.1* in induced roots based on real-time RT-PCR cycle number comparisons (data not shown). *AtNRT1.1* expression level in wild-type shoots was higher than roots at 0 h, and showed a slight induction by KNO_3, whereas *AtNRT2.1* expression levels were <1% of roots but were induced significantly by 3 h. Similarly both *NRT* genes were strongly induced by KNO_3 in the *Atnrt3.1* mutant roots, indicating that the defect in *AtNRT3.1*

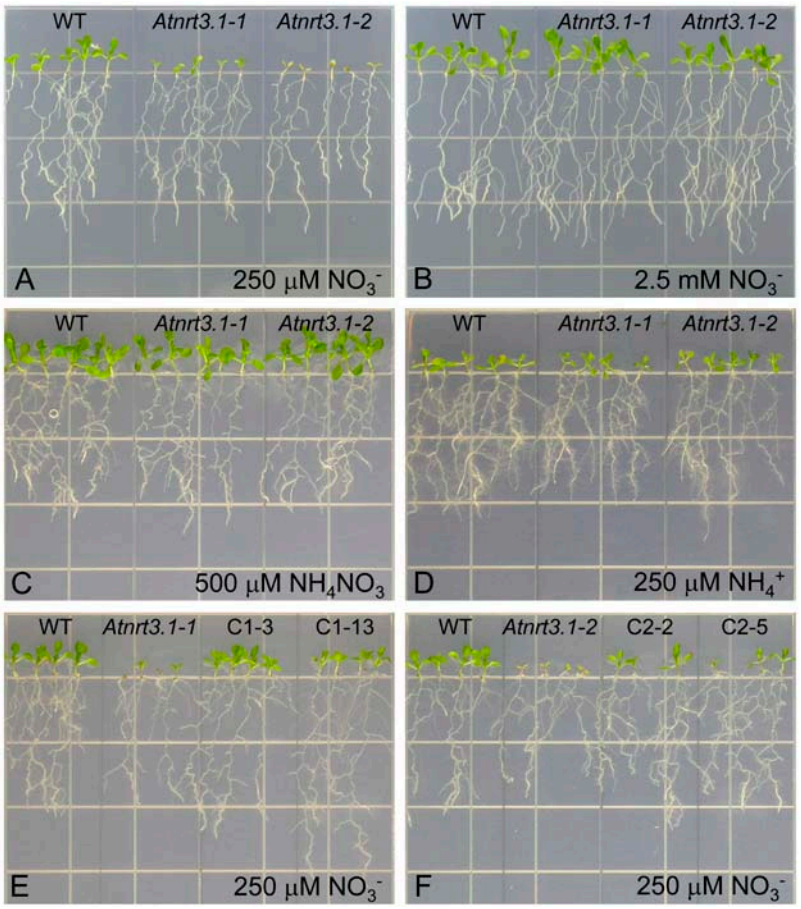

Figure 3. Plant growth on various nitrogen sources. A to D, Wild-type plants and *Atnrt3.1* mutants were grown on vertical plates containing 250 μM KNO_3 (A), 2.5 mM KNO_3 (B), 500 μM NH_4NO_3 (C), or 125 μM $(NH_4)_2$ succinate (D) with other nutrients for 10 d. E and F, Complemented lines (C1-3, C1-13, C2-2, and C2-5) with *35S-NRT3.1* in the *Atnrt3.1-1* (E) and *Atnrt3.1-2* (F) mutant background were grown in 250 μM KNO_3 for 10 d.

did not prevent induction of these nitrate transporter genes at the transcriptional level. Nevertheless, the expression levels of both *AtNRT1.1* and *AtNRT2.1* in the mutants were significantly lower than those in wild type. *AtNRT1.1* levels in *Atnrt3.1-1* and *Atnrt3.1-2* peaked with 8- and 4-fold induction, respectively, giving expression levels that were 50% and 75% lower than wild type, respectively. *AtNRT2.1* was induced about 20-fold in both mutants. However, the expression levels were also lower than wild type in the same order (wild type > *Atnrt3.1-1* > *Atnrt3.1-2*) at all time points. In shoots of the mutants, *AtNRT1.1* levels were similar to wild type, whereas *AtNRT2.1* levels remained low and showed a small induction (Fig. 4, C and D).

Tissue Nitrate Analysis

To determine tissue NO_3^- accumulation during the standard induction period (i.e. 6 h pretreatment in 1 mM KNO_3, as used for the gene expression analyses described above), root and shoot samples of wild-type and *Atnrt3.1-2* mutant plants were weighed, boiled in distilled water for 5 min, and tissue NO_3^- concentrations determined by the Cataldo method (Cataldo et al., 1975). As shown in Table II, wild-type roots and shoots accumulated significantly more NO_3^- than mutant during 6 h, specifically 5.4-fold higher in wild-type roots (7.5 μmol g^{-1} FW versus 1.4 μmol g^{-1} FW increases in wild type and mutant, respectively), and 52-fold more in wild-type shoots (5.2 μmol g^{-1} FW versus 0.1 μmol g^{-1} FW increases in wild type and mutant, respectively).

High-Affinity Nitrate Influx

High-affinity nitrate influx into intact roots of wild-type and mutant plants was examined using $^{13}NO_3^-$ to

Table I. *Shoot and root FWs and shoot:root ratios in wild-type and Atnrt3.1 mutants*

Plants were grown for 4 weeks in 1 mM NH_4NO_3 and then nitrogen deprived for 1 week. The values are the means of five (wild type) or 12 (*Atnrt3.1* mutants) plants ± SE. Differences between wild-type and mutant shoot weights and shoot:root ratios were highly significant ($P > 0.05$, *t* test).

Genotype	FW		Shoot:Root Ratio
	Shoot	Root	
	g plant^{-1}		
Wild type	0.46 ± 0.03	0.13 ± 0.02	3.5
Atnrt3.1-1	0.23 ± 0.02	0.17 ± 0.05	1.4
Atnrt3.1-2	0.15 ± 0.03	0.10 ± 0.03	1.5

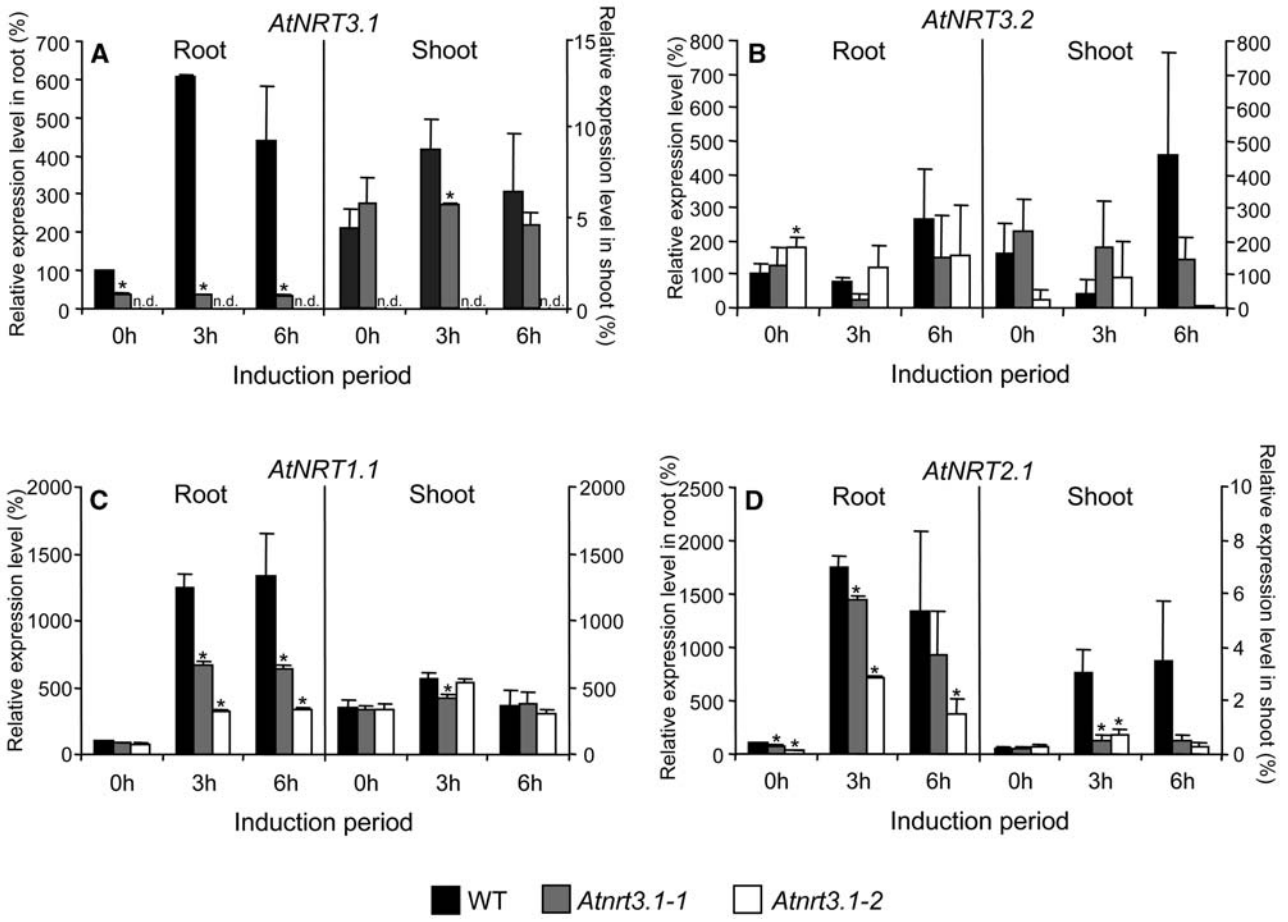

Figure 4. Expression analysis of *AtNRT3, AtNRT1.1*, and *AtNRT2.1* genes in response to nitrate by relative quantitative real-time RT-PCR. A to D, Plants were grown for 4 weeks in 1 mM NH_4NO_3 and then nitrogen deprived for 1 week before being reexposed to 1 mM KNO_3 for 0, 3, and 6 h. Each sample was normalized by clathrin and relatively expressed to wild-type root at 0 h. Relative expression values of *AtNRT3.1* (A), *AtNRT3.2* (B), *AtNRT1.1* (C), and *AtNRT2.1* (D) are means of four replicates (two biological replicates × two independent reactions). Error bars = SE. Asterisk (*) indicates significant difference of the mutants from wild type (*t* test, $P < 0.05$). n.d. indicates the following levels: root (<0.3%) and shoot (0%).

determine the effect of the *Atnrt3.1* mutations. Figure 5A shows high-affinity nitrate influx into roots of wild-type and *Atnrt3.1-2* mutant plants, measured at external NO_3^- concentrations from 10 to 150 μM. In this experiment, plants were grown for 4 weeks in 1 mM NH_4NO_3 and then transferred to solutions without nitrogen for 7 d before being reexposed to 1 mM KNO_3. This treatment has previously been shown to deinduce IHATS and ensure that root NO_3^- stores are consumed (Okamoto et al., 2003). Subsequently, the provision of 1 mM KNO_3 for 6 h to plants pretreated in this fashion, caused *AtNRT2.1* transcript and high-affinity nitrate influx to reach peak values within 3 and 6 h, respectively. Thereafter, transcript abundance and influx gradually decline (Okamoto et al., 2003). Compared to wild-type plants, nitrate influx into roots of mutant plants was reduced across the whole range of NO_3^- concentration examined. V_{max} values for wild-type and mutant plants were 8.3 ± 0.7 and 0.2 ± 0.1 μmol g FW^{-1} h^{-1}, respectively, while corresponding K_m values were 60 ± 11 and 129 ± 65 μM. The V_{max} for influx was reduced by 98%. Similar results were obtained with *Atnrt3.1-1* mutant plants (data not shown), however the high-affinity influx was reduced by only 80% in this mutant. To determine the component fluxes (CHATS and IHATS) of the measured high-affinity influx it is necessary to measure influx in uninduced plants. Thus, influx was also measured in nitrate-deprived

Table II. *Tissue nitrate concentration in wild type and the Atnrt3.1-2 mutant*

Plants were grown for 4 weeks in 1 mM NH_4NO_3 and then nitrogen deprived for 1 week. Nitrate contents (μmol g^{-1} FW) were then measured at time 0 (0 h) and after 6 h of incubation with 1 mM KNO_3. The values are the means of five plants ± SE. Differences between wild-type and mutant root or shoot were significant at 6 h ($P > 0.05$, *t* test).

Genotype	Treatment (1 mM KNO_3)	Root	Shoot
Wild type	0 h	0.38 ± 0.1	5.0 ± 0.1
	6 h	7.9 ± 0.2	10.2 ± 0.2
Atnrt3.1-2	0 h	0.3 ± 0.1	6.3 ± 0.15
	6 h	1.7 ± 0.1	6.4 ± 0.1

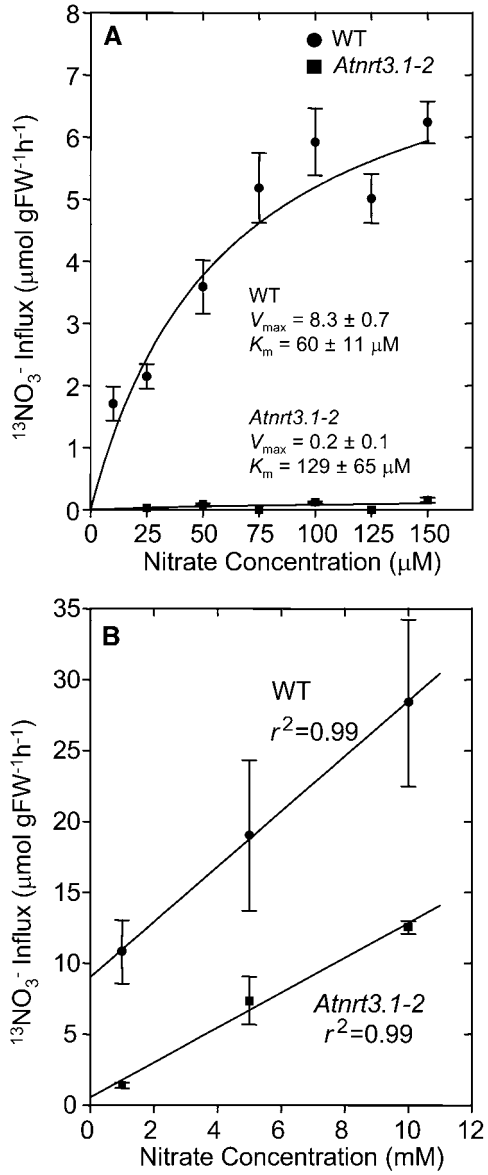

Figure 5. $^{13}NO_3^-$ influx into wild-type and *Atnrt3.1-2* mutant roots. A, High-affinity $^{13}NO_3^-$ influx. Plants were grown for 4 weeks in 1 mM NH_4NO_3 and then nitrogen deprived for 1 week before being reexposed to 1 mM KNO_3 for 6 h. Nitrate influx was then measured at 10, 25, 50, 75, 100, 125, and 150 μM NO_3^- as described in "Materials and Methods." Data values are means ± SE of five replicates. The fitted curve was obtained by direct fit to the Michaelis-Menten equation. Estimated K_m and V_{max} values are indicated in the figure. B, Low-affinity $^{13}NO_3^-$ influx. Plants were grown for 4 weeks in 1 mM NH_4NO_3 and then nitrogen deprived for 1 week before being reexposed to 1 mM KNO_3 for 6 h. Nitrate influx was then measured at 1, 5, and 10 mM NO_3^-. Data values are means ± SE of four replicates.

plants during the first 10 min of exposure to 100 μM KNO_3 after 7 d of nitrogen deprivation. The results of this experiment are shown in Figure 6A as percentages of the wild-type fluxes. Absolute influx values before induction were 1.9 ± 0.1 μmol g FW^{-1} h^{-1} (wild type) and 1.26 ± 0.1 (*Atnrt3.1-1* mutant), respectively, a reduction of 34%. In separate experiments corresponding values for wild type and the *Atnrt3.1-2* mutant were 2.7 ± 0.4 and 0.3 ± 0.1 μmol g FW^{-1} h^{-1}, respectively, a reduction of 89%. Using the same batch of plants, $^{13}NO_3^-$ was measured after 6 h of exposure to 1 mM KNO_3. The measured fluxes (CHATS plus IHATS) had increased to 9.84 ± 1.0 μmol g FW^{-1} h^{-1} in wild-type roots, 1.9 ± 0.32 in the *Atnrt3.1-1* mutant, and 0.32 ± 0.2 μmol g FW^{-1} h^{-1} in the *Atnrt3.1-2* mutant. Thus, IHATS influx (measured flux in induced plants minus that of uninduced plants) was reduced by 92% and 96% in the *Atnrt3.1-1* and *Atnrt3.1-2* mutants, respectively (Fig. 6B).

Low-Affinity Nitrate Influx

To determine if the low value of influx in the mutant plants was due in part to disruption of the LATS influx, $^{13}NO_3^-$ influx into roots of both lines of mutant plants, deprived of nitrate for 7 d, and then exposed to 1 mM KNO_3 for 6 h, was determined from solutions containing 1, 5, and 10 mM $K^{13}NO_3$ (Fig. 5B). In both lines $^{13}NO_3^-$ influx in the LATS concentration range was found to be unaffected by the *AtNRT3.1* mutation, except that measured fluxes at all three concentrations were reduced by the extent to which the IHATS flux had been reduced. Data for the *Atnrt3.1-2* mutant line

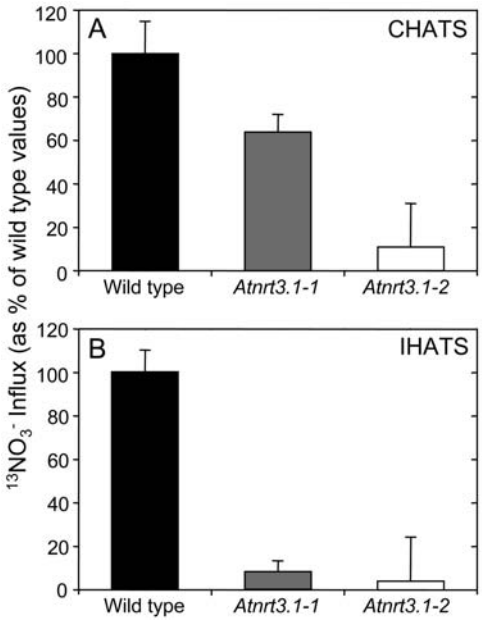

Figure 6. $^{13}NO_3^-$ influx by CHATS and IHATS. A, $^{13}NO_3^-$ influx due to CHATS in wild-type and *Atnrt3.1* mutants as percentages of wild-type fluxes. Plants were grown for 4 weeks in 1 mM NH_4NO_3 and then nitrogen deprived for 1 week. Nitrate influx was then measured at 100 μM NO_3^-. B, $^{13}NO_3^-$ influx due to IHATS in wild-type and *Atnrt3.1* mutants as percentages of wild-type fluxes. Plants were grown for 4 weeks in 1 mM NH_4NO_3 and then nitrogen deprived for 1 week before being reexposed to 1 mM KNO_3 for 6 h. Nitrate influx was then measured at 100 μM NO_3^-. IHATS influxes were calculated by subtracting the measured CHATS flux from the flux measured after induction. Data values are means ± SE of four replicates.

is shown in Figure 5B. Results for the *Atnrt3.1-1* mutant (data not shown) were essentially identical to those for *Atnrt3.1-2*.

DISCUSSION

The goal of this study was to determine if high-affinity nitrate transport into roots of Arabidopsis requires the presence of a functional *NAR2*-like gene (i.e. *AtNRT3*) in addition to members of the *NRT2* family. A requirement for the presence of functional *AtNRT2.1* and *AtNRT2.2* genes was established previously by demonstrating that inducible high-affinity nitrate influx in a T-DNA mutant disrupted in *AtNRT2.1* and *AtNRT2.2* was strongly impaired compared to control plants (Cerezo et al., 2001; Filleur et al., 2001). The same study revealed that low-affinity influx was unaffected by this disruption.

Expression Patterns of *AtNRT3* and *AtNRT2.1* Genes

The absence of ESTs for *AtNRT3.2* and the present expression analyses of *AtNRT3.1* and *AtNRT3.2* suggest that only *AtNRT3.1* would be detected under the conditions examined. The pattern of expression of *AtNRT3.1* is quite similar, with respect to induction by nitrate, to *AtNRT2.1*, which is thought to encode an inducible high-affinity nitrate transporter (Zhuo et al., 1999; Cerezo et al., 2001; Filleur et al., 2001; Okamoto et al., 2003). In the *Atnrt3.1* T-DNA mutant plants, *AtNRT3.1* transcript levels were low or virtually undetectable compared to wild-type plants deprived of nitrate (Fig. 4). After exposure to 1 mM KNO_3 to induce expression of nitrate-inducible genes, *AtNRT3.1* transcript abundance actually declined in the *Atnrt3.1-1* mutant. By contrast *AtNRT3.1* transcript abundance increased 6-fold in wild-type plants during the first 3 h after resupply of 1 mM KNO_3, and tended to decline by 6 h. This decline was observed to continue until 24 h had elapsed, when the expression level was down to preinduced level (data not shown). This pattern of *AtNRT3.1* expression in wild-type plants following reexposure to KNO_3 is similar to that of *AtNRT2.1*, which typically peaks in abundance after 3 h then declines (Fig. 4; see Zhuo et al., 1999; Okamoto et al., 2003).

In this study, *AtNRT2.1* abundance in roots of the *Atnrt3.1-1* and *Atnrt3.1-2* mutants increased approximately 13- and 6-fold, respectively, after reexposure to 1 mM KNO_3 (Fig. 4D), demonstrating that *AtNRT3.1* is not required for transcription of *AtNRT2.1*. We also examined expression patterns of *AtNRT1.1* (*CHL1*), another nitrate-inducible gene encoding the inducible dual-affinity nitrate transporter. Transcript abundances increased as a result of this protocol both in the *Atnrt3.1* mutants and wild-type plants, although the extent of inductions were less in the mutants as seen in *AtNRT2.1* (Fig. 3C). The most likely cause of reduced expression of these nitrate-induced genes is the reduced root NO_3^- concentration associated with disruption of high-affinity nitrate influx. Indeed, as demonstrated in the "Results" section, $^{13}NO_3^-$ influx into roots of mutant plants and tissue NO_3^- concentration were substantially reduced compared to wild-type plants (Figs. 5 and 6; Table II). Indeed, the opposite result, namely elevated levels of *NRT2.1* transcript, have been reported in nitrate reductase (NR) mutants or in plants treated with tungstate to block NR activity, due to elevated tissue NO_3^- concentration in the absence of downstream products of nitrate assimilation (Filleur and Daniel-Vedele, 1999; Vidmar et al., 2000). If this interpretation is correct, it suggests that induction of nitrate-dependent genes requires the entry of nitrate into the roots rather than external sensing of nitrate, a hypothesis that has been suggested earlier (Unkles et al., 2001), because roots of mutant plants were exposed to the same NO_3^- concentration as wild-type plants during induction.

There are examples where one gene in a gene family can compensate for the loss of other homologous gene(s). Examples of this functional compensation include the phosphate transporter *PHO* family in *Saccharomyces cerevisiae* (Wykoff and O'Shea, 2001) and the ammonium transporter *AMT* family in Arabidopsis (Kaiser et al., 2002). In this study, however, *AtNRT3.2* failed to compensate for the disrupted *AtNRT3.1* gene in the mutant, since *AtNRT3.2* (normally expressed at substantially lower levels than *AtNRT3.1*) showed no apparent sign of nitrate induction in either wild-type or the *Atnrt3.1* mutants.

Nitrate Influx

The first indication that high-affinity nitrate uptake was disrupted in the *Atnrt3.1* mutants was the poor growth on low-nitrate media (Fig. 3A). In particular, shoot growth was impaired. This was confirmed quantitatively in plants used for influx studies that had been grown on 1 mM NH_4NO_3 under hydroponic conditions. Shoot-to-root ratios were strongly reduced in mutant plants, even though 50% of nitrogen came from NH_4^+ (Table I). Such low shoot-to-root ratios are typical of nitrogen deprivation. By contrast, mutant growth was restored to wild-type levels when plants were grown on elevated concentrations of KNO_3, or on $(NH_4)_2$ succinate. Normalization of plant growth on 2.5 mM NO_3^- in agar suggests that influx via the LATS (which was shown to function normally in the *Atnrt3.1* mutants, see below) was sufficient to satisfy plant demand. Likewise, growth was normalized in the mutant lines that had been rescued with an *AtNRT3.1* cDNA (Fig. 3, E and F).

To evaluate the role of *AtNRT3* in high-affinity nitrate influx directly, plants that had been maintained on 1 mM NH_4NO_3 for 4 weeks were completely deprived of nitrate for 7 d and then reexposed to 1 mM KNO_3 for 6 h to induce expression of nitrate-inducible genes. NH_4NO_3 was used in the prior growth period to optimize growth, especially that of mutant plants that

exhibited impaired growth on KNO_3 as the sole source of nitrogen. However, in the standard induction NH_4^+ was omitted since it is well known to inhibit nitrate influx. $^{13}NO_3^-$ influx was then measured using various concentrations of KNO_3 before and after the 6 h period of induction. The data presented in Figure 5A show that disruption of *AtNRT3.1* caused a virtual elimination of high-affinity influx in nitrate-induced plants across the whole range of NO_3^- concentration investigated. Influx values before induction (at time 0 h), presumably due to the CHATS alone or in combination with a CLATS, were also reduced but to different extents in the two mutant lines. Expressing wild-type fluxes as 100%, the reductions of CHATS associated with the T-DNA insertion were 34% in the *Atnrt3.1-1* mutant and 89% in the *Atnrt3.1-2* mutant. These results indicate that the *AtNRT3.1* gene is required not only for normal activity of the IHATS but also for the CHATS. The relatively small reduction of CHATS in the *Atnrt3.1-1* mutant may be the result of leakiness in this mutation associated with the location of the disruption in the promoter region of *AtNRT3.1*. The influx values for wild-type plants are similar to those reported in earlier studies for nitrate-deprived Arabidopsis roots (Zhuo et al., 1999; Okamoto et al., 2003). Following induction, $^{13}NO_3^-$ influx increased from 1.9 ± 0.1 to 9.84 ± 1.0 μmol g FW^{-1} h^{-1} in wild-type plants, from 1.26 ± 0.1 to 1.90 ± 0.1 μmol g FW^{-1} h^{-1} in the *Atnrt3.1-1* mutant, and from 0.3 ± 0.1 to 0.32 ± 0.2 in the *Atnrt3.1-2* mutant. Thus the inducible component of HATS influx (IHATS: measured flux in induced plants minus that of uninduced plants) was reduced by 92% and 96% in the *Atnrt3.1-1* and *Atnrt3.1-2* mutant lines, respectively (Fig. 6B). Again, we suggest that the small increase of influx in the *Atnrt3.1-1* mutant (from 1.26–1.90 μmol g FW^{-1} h^{-1}) may have been due to a leaky mutation in this line. By contrast, the large increase in wild-type plants after reexposure to NO_3^- (from 1.9–9.84 μmol g FW^{-1} h^{-1}) represents the combined contribution of the large IHATS influx together with any contribution from the ILATS.

It is evident from the foregoing discussion that the IHATS is essentially absent in the *Atnrt3.1* mutants, but (as stated above) it was possible that the ILATS and/or the CLATS might also have contributed to the calculated IHATS and have a requirement for coexpression of *AtNRT3.1*. To evaluate this possibility, $^{13}NO_3^-$ influx was measured in wild-type and the *Atnrt3.1* mutant plants at 1, 5, and 10 mM KNO_3, concentrations that are typical of the LATS. Figure 5B indicates an essentially normal concentration response of the *Atnrt3.1-2* mutant plants, suggesting that LATS function is not disrupted in these plants, and does not require coexpression of *AtNRT3.1*. The absolute value of influx was lower in the case of the mutants because IHATS function had been disrupted. Note that the intercept values for influx correspond quite closely to the values obtained for HATS influx measured at 100 μM. Identical results were obtained for *Atnrt3.1-1* mutant (data not shown).

In summary, this study establishes that Arabidopsis possesses two *NAR2*-like genes, *AtNRT3.1* and *AtNRT3.2*. Of these only *AtNRT3.1* is expressed at significant levels and *AtNRT3.1* proved to be highly responsive to induction by nitrate. In the *Atnrt3.1* mutants described, *AtNRT3.1* transcript was expressed at very low levels compared to the wild type and was not induced by exposure to nitrate. In these mutants, both high-affinity nitrate transport systems (CHATS and IHATS) are functionally impaired, even though transcript abundance of *AtNRT2.1* was strongly expressed after induction. Therefore, in Arabidopsis both the CHATS and the IHATS appear to require coexpression of the *AtNRT3.1* gene. By contrast, LATS function was shown to be independent of the *AtNRT3.1* expression.

MATERIALS AND METHODS

Plant Growth Conditions and Influx Determinations

Plants used for gene expression and influx studies were maintained in an environment chamber with light/dark periods of 8/16 h, 25°C/20°C, and relative humidity = 70%, with photon flux of 150 to 200 μE m^{-2} s^{-1}. Plants were grown hydroponically in nutrient solution with 1 mM KH_2PO_4, 0.5 mM $MgSO_4$, 0.25 mM $CaSO_4$, 20 μM Fe-EDTA, 25 μM H_3BO_3, 2 μM $ZnSO_4$, 2 μM $MnSO_4$, 0.5 μM $CuSO_4$, and 0.5 μM $(NH_4)_6Mo_7O_{24}$ in 8-L plastic containers. The pH of the nutrient solution was maintained with $CaCO_3$ around 6.2 for all the experiments. One-centimeter holes were cut in Styrofoam platforms (1.25 cm thickness) and nylon mesh was placed over the holes. Fine sand was placed in the mesh and seeds were planted on top of the sand. The platforms and seeds were then floated on the nutrient solutions. After seeding onto the platform, seeds were imbibed in a cold room at 4°C for 3 to 4 d.

For the nitrate influx analyses through HATS, plants were grown at 1 mM NH_4NO_3 for 4 weeks and then transferred to media lacking any source of nitrogen for 1 week. To measure CHATS activity roots of plants were transferred to fresh medium containing 100 μM KNO_3 for 5 min before being exposed to chemically identical solutions, except that the KNO_3 was labeled with $^{13}NO_3^-$. After exposure to tracer for 5 min, roots were transferred back to identical nonlabeled solutions for 3 min to desorb tracer from the cell walls. To measure induced fluxes, plants were grown on 1 mM NH_4NO_3 for 4 weeks, transferred to −N solution for 1 week, and then reinduced with 1 mM KNO_3 for up to 6 h. Roots of plants used for experiments designed to measure concentration-dependent fluxes were induced in the same manner as described above and then roots were pretreated for 5 min at the concentration to be used to measure tracer fluxes. The same standard desorption protocol (described above) was used in these experiments. After desorption, roots and shoots were separated, weighed, and put into vials for counting using a γ-counter (MINAXI Auto-Gamma 5000 series, Packard Instruments). Generation and purification of $^{13}NO_3^-$ and other details regarding influx analyses using $^{13}NO_3^-$ are described by Siddiqi et al. (1989).

Continuous light was provided for the growth study on plates. The nutrient medium was the same as described above except for nitrogen whose concentration was as indicated in the figures. In addition, the nutrient solution contained 0.5% (w/v) Suc and 0.5 g/L of MES (pH 5.7), and 0.7% (w/v) agarose (Invitrogen).

Isolation of *Atnrt3.1* Mutant Lines

The *Atnrt3.1-1* mutant was isolated from a population of 60,480 T-DNA inserted lines (Ws background) from the Arabidopsis knockout facility at the University of Wisconsin. The methodology was described by Krysan et al. (1996, 1999). Primers from the right border of the T-DNA (XR-2: 5′-TGGGAAAACCTGGCGTTACCCAACTTAAT), and from *AtNRT3.1* (forward: 5′-CTCTTCTCTTCCTCAGCCTTATTTTTCTG, reverse: 5′-GAAGAAGTGTGCAACAAGACAAAAGGAAT) were used for the PCR-based screening and the subsequent genotyping. During the screening, putative PCR products were also verified by Southern-blot analysis using 1.1 kb *AtNRT3.1* genomic DNA fragment (a PCR product of the *AtNRT3.1* forward and reverse

primers above) as a probe (data not shown). PCR products, which also showed positive in the Southern-blot analysis, were cloned into TOPO TA cloning vector (Invitrogen) and sequenced.

The *Atnrt3.1-2* mutant was identified in the FLAGdb T-DNA lines (Samson et al., 2002). Primer sets for the T-DNA (left border: 5′-TCCAGGGCGTGTGCCAGGTGC, right border: 5′-CCAGACTGAATGCCCACAGGCCGTC) and for *AtNRT3.1* (forward: 5′-AGCCAAGTTGACCGACCATGG, reverse: 5′-GATTTCTCTTTGAAAGTAAGAGGTGAAG) were used for PCR-based genotyping and sequencing of the T-DNA/genome flanking region.

Quantitative Real-Time PCR

To determine T-DNA copy number in the mutant lines, genomic DNA was isolated from mature leaves of homozygous *Atnrt3.1* mutants by DNeasy plant mini kit (Qiagen) and analyzed by quantitative real-time PCR assay (Ingham et al., 2001). Primers were designed specific to *GUS* and nitrite reductase (AGI code: At2g15620) for transgene and endogenous control gene, respectively. As a control line we included a transgenic plant in which the *GUS* gene copy number had already been determined (M. Galli, unpublished data). Quantitative real-time PCR was performed by using LightCycler (Roche) with the SYBR Green I detection system, under the following conditions: 95°C for 10 min; 45 cycles of 95°C for 5 s, 63°C for 5 s, and 72°C for 10 s; followed by melting curve analysis. PCR mixture of a final volume of 10 μL contained 2 μL of gDNA, 0.5 μM of each primer, 4 mM Mg^{2+}, and 1 μL of LightCycler-FastStart DNA Master SYBR Green I mixture (Roche). The following primer sets were used: *GUS* (forward: 5′-CGTTTCGATGCGGTCACTC; reverse: 5′-CGTCGGTAATCACCATTCCC) and NR (forward: 5′-CCGGTAGCCAGTTCTGCG; reverse: 5′-CCTATTCGTCCCCCGACGT).

For gene expression analysis total RNA was isolated from approximately 100 mg FW with RNeasy plant mini kit (Qiagen). RNase-free DNase treatment was also carried out during the isolation. Gene expression levels were analyzed by two-step real-time RT-PCR. cDNAs were synthesized from 250 ng of total RNA by Transcriptor (Roche), and the reaction mixture was diluted 20 times for subsequent PCR. The conditions for the quantitative real-time PCR were same as above. As a control, no RT (omitting reverse transcriptase in RT step) reaction was included. PCR mixture of a final volume of 10 μL contained 2 μL of cDNA, 0.5 μM of each primer, and 2 μL of LightCycler-FastStart DNA Plus Master SYBR Green I mixture (Roche). The following primer sets were used: *AtNRT3.1* (forward: 5′-GACCTGCCCACACAAGATCA; reverse: 5′-TGGAGGCAATATCTAGGGACGC); *AtNRT3.2* (forward: 5′-CATGAGATTGTGTCCAAGGCATA; reverse: 5′-TATGTCTAGCCCCACGTGATGA); *AtNRT1.1* (forward: 5′-AAAGCTGCCACACACTGAAC; reverse: 5′-ATTGTGCGACTGATAATGTCGT); *AtNRT2.1* (forward: 5′-CCACAGATCCAGTGAAAGG; reverse: 5′-CATTGTTGGGTGTGTTCTCA); and Clathrin-At4g24550 (internal control gene; forward: 5′-ATACGCGCTGAGTTCCC; reverse: 5′-CTGACTGGCCCTGCTT). Quantitative data analysis was performed with the LightCycler software 4.0 (Roche).

Rescue of the *Atnrt3.1* Mutants

To rescue the *Atnrt3.1* mutants the *AtNRT3.1* cDNA driven by the CaMV 35S promoter was transformed into the mutant plants. First, the cDNA *AtNRT3.1* was amplified by RT-PCR from wild-type (Ws) root total RNA using a pair of primers (forward: 5′-AAGGATCCATGGCGATCCAGAAGA; reverse: 5′-TCCCGGGTAAACGACTCATTTGCTTTGCT), introducing *Bam*HI and *Sma*I sites at 5′ and 3′ ends of the cDNA, respectively. The PCR product was cloned into pGEM-Teasy (Promega) and sequenced to check its integrity. The *NRT3.1* *Bam*HI/*Sma*I fragment was cloned into the *Bam*HI/*Sma*I sites of two binary vectors, the pGreen0229 (Hellens et al., 2000) in which the CaMV 35S-cassette was introduced, and the pBIN-JIT (Kwak et al., 2001), designated as pGreen-NRT3.1 and pBIN-JIT-NRT3.1, respectively. The pBIN-JIT-NRT3.1 was then partially digested with *Kpn*I and *Hin*dIII to produce an approximately 2.5-kb fragment of the 35S promoter-*NRT3.1* terminator cassette. The DNA cassette was cloned into the pCAMBIA1303 binary vector (CAMBIA) at the *Kpn*I/*Hin*dIII sites (designated as pCAMBIA-NRT3.1). The pGreen-NRT3.1 and pCAMBIA-NRT3.1 were transformed into *Atnrt3.1-1* and *Atnrt3.1-2* mutant lines, respectively, by the floral-dip procedure (Clough and Bent, 1998) with *Agrobacterium tumefaciens* strain C58. Transformants were selected either in pots by spraying with 300 μM glufosinate ammonium for the pGreen-NRT3.1, or on Murashige and Skoog plates containing 27 μg/mL hygromycin (A.G. Scientific) for the pCAMBIA-NRT3.1. More than six transgenic lines that showed 3:1 ratio to the selection markers in the T_2 generation were characterized, and two representative lines for each vector were presented in this paper.

ACKNOWLEDGMENTS

We thank the Tri-University Meson Facility at the University of British Columbia for the provision of ^{13}N, and Mary Galli for providing T-DNA lines.

Received November 18, 2005; revised January 3, 2006; accepted January 9, 2006; published January 13, 2006.

LITERATURE CITED

Arabidopsis Genome Initiative (2000) Analysis of the genome sequence of the flowering plant *Arabidopsis thaliana*. Nature **408:** 796–815

Cataldo DA, Haroon M, Schrader LE, Youngs VL (1975) Rapid colorimetric determination of nitrate in plant tissue by nitration of salicylic acid. Commun Soil Sci Plant Anal **6:** 71–80

Cerezo M, Tillard P, Filleur S, Munos S, Daniel-Vedele F, Gojon A (2001) Major alterations of the regulation of root NO_3^- uptake are associated with the mutation of *Nrt2.1* and *Nrt2.2* genes in Arabidopsis. Plant Physiol **127:** 262–271

Clough SJ, Bent AF (1998) Floral dip: a simplified method for Agrobacterium-mediated transformation of Arabidopsis thaliana. Plant J **16:** 735–743

Crawford NM, Glass ADM (1998) Molecular and physiological aspects of nitrate uptake in plants. Trends Plant Sci **3:** 389–395

Filleur S, Daniel-Vedele F (1999) Expression analysis of a high-affinity nitrate transporter isolated from *Arabidopsis thaliana* by differential display. Planta **207:** 461–469

Filleur S, Dorbe MF, Cerezo M, Orsel M, Granier F, Gojon A, Daniel-Vedele F (2001) An *Arabidopsis* T-DNA mutant affected in *Nrt2* genes is impaired in nitrate uptake. FEBS Lett **489:** 220–224

Forde BG (2000) Nitrate transporters in plants: structure, function and regulation. Biochim Biophys Acta **1465:** 219–235

Hellens RP, Edwards EA, Leyland NR, Bean S, Mullineaux PM (2000) pGreen: a versatile and flexible binary Ti vector for *Agrobacterium*-mediated plant transformation. Plant Mol Biol **42:** 819–832

Ingham DJ, Beer S, Money S, Hansen G (2001) Quantitative real-time PCR assay for determining transgene copy number in transformed plants. Biotechniques **31:** 132–140

Kaiser BN, Rawat SR, Siddiqi MY, Masle J, Glass ADM (2002) Functional analysis of an Arabidopsis T-DNA ''knockout'' of the high-affinity NH_4^+ transporter AtAMT1;1. Plant Physiol **130:** 1263–1275

Krogh A, Larsson B, von Heijne G, Sonnhammer ELL (2001) Predicting transmembrane protein topology with a hidden Markov model: application to complete genomes. J Mol Biol **305:** 567–580

Krysan PJ, Young JC, Sussman MR (1999) T-DNA as an insertional mutagen in Arabidopsis. Plant Cell **11:** 2283–2290

Krysan PJ, Young JC, Tax F, Sussman MR (1996) Identification of transferred DNA insertions within *Arabidopsis* genes involved in signal transduction and ion transport. Proc Natl Acad Sci USA **93:** 8145–8150

Kwak JM, Murata Y, Baizabal-Aguirre VM, Merrill J, Wang M, Kemper A, Hawke SD, Tallman G, Schroeder JI (2001) Dominant negative guard cell K^+ channel mutants reduce inward-rectifying K^+ currents and light-induced stomatal opening in Arabidopsis. Plant Physiol **127:** 473–485

Liu KH, Huang CY, Tsay YF (1999) CHL1 is a dual-affinity nitrate transporter of Arabidopsis involved in multiple phases of nitrate uptake. Plant Cell **11:** 865–874

Liu KH, Tsay YF (2003) Switching between the two action modes of the dual-affinity nitrate transporter CHL1 by phosphorylation. EMBO J **22:** 1005–1013

Nakai K, Kanehisa M (1992) A knowledge base for predicting protein localization sites in eukaryotic cells. Genomics **14:** 897–911

Nazoa P, Vidmar JJ, Tranbarger TJ, Mouline K, Damiani I, Tillard P, Zhuo DG, Glass ADM, Touraine B (2003) Regulation of the nitrate transporter gene *AtNRT2.1* in *Arabidopsis thaliana*: responses to nitrate, amino acids and developmental stage. Plant Mol Biol **52:** 689–703

Nielsen H, Brunak S, von Heijne G (1999) Machine learning approaches for the prediction of signal peptides and other protein sorting signals. Protein Eng **12:** 3–9

Okamoto M, Vidmar JJ, Glass ADM (2003) Regulation of *NRT1* and *NRT2* gene families of *Arabidopsis thaliana*: responses to nitrate provision. Plant Cell Physiol **44:** 304–317

Quesada A, Galvan A, Fernandez E (1994) Identification of nitrate transporter genes in *Chlamydomonas reinhardtii.* Plant J **5:** 407–419

Samson F, Brunaud V, Balzergue S, Dubreucq B, Lepiniec L, Pelletier G, Caboche M, Lecharny A (2002) FLAGdb/FST: a database of mapped flanking insertion sites (FSTs) of *Arabidopsis thaliana* T-DNA transformants. Nucleic Acids Res **30:** 94–97

Siddiqi MY, Glass ADM, Ruth TJ, Fernando M (1989) Studies of the regulation of nitrate influx by barley seedlings using $^{13}NO_3^-$. Plant Physiol **90:** 806–813

Tong Y, Zhou JJ, Li ZS, Miller AJ (2005) A two-component high-affinity nitrate uptake system in barley. Plant J **41:** 442–450

Trueman LJ, Richardson A, Forde BG (1996) Molecular cloning of higher plant homologues of the high-affinity nitrate transporters of *Chlamydomonas reinhardtii* and *Aspergillus nidulans.* Gene **175:** 223–231

Tsay YF, Schroeder JI, Feldmann KA, Crawford NM (1993) The herbicide sensitivity gene *CHL1* of Arabidopsis encodes a nitrate-inducible nitrate transporter. Cell **72:** 705–713

Unkles SE, Hawker KL, Grieve C, Campbell EI, Montague P, Kinghorn JR (1991) *crnA* encodes a nitrate transporter in *Aspergillus nidulans.* Proc Natl Acad Sci USA **88:** 204–208

Unkles SE, Zhou D, Siddiqi MY, Kinghorn JR, Glass ADM (2001) Apparent genetic redundancy facilitates ecological plasticity for nitrate transport. EMBO J **20:** 6246–6255

Vidmar JJ, Zhuo D, Siddiqi MY, Schjoerring JK, Touraine B, Glass ADM (2000) Regulation of high-affinity nitrate transporter genes and high-affinity nitrate influx by nitrogen pools in roots of barley. Plant Physiol **123:** 307–318

Wang R, Liu D, Crawford NM (1998) The *Arabidopsis* CHL1 protein plays a major role in high-affinity nitrate uptake. Proc Natl Acad Sci USA **95:** 15134–15139

Wykoff DD, O'Shea EK (2001) Phosphate transport and sensing in *Saccharomyces cerevisiae.* Genetics **159:** 1491–1499

Zhou JJ, Fernandez E, Galvan A, Miller AJ (2000) A high affinity nitrate transport system from *Chlamydomonas* requires two gene products. FEBS Lett **466:** 225–227

Zhuo DG, Okamoto M, Vidmar JJ, Glass ADM (1999) Regulation of a putative high-affinity nitrate transporter (*Nrt2;1At*) in roots of *Arabidopsis thaliana.* Plant J **17:** 563–568